Supporting Information

Au@*h*-Al_2O_3 analogic yolk-shell nanocatalyst for highly selectively synthesis of biomass-derived $_D$-xylonic acid via regulation of structure effect

Jiliang Ma,[a] Zewei Liu,[a,c] Junlong Song,[b] Linxin Zhong,[a] Dequan Xiao,[d] Hongxia Xi,[c] Xuehui Li,[c] Runcang Sun *[e] and Xinwen Peng *[a]*

Materials: Styrene (99%), potassium persulfate ($K_2S_2O_8$), hydrochloric acid (HCl, 36%-38%), sodium hydroxide (NaOH), magnesium sulfate ($MgSO_4$), sodium borohydride ($NaBH_4$, ≥97%), ammonium formate, formic acid, aluminum sulfate ($Al_2(SO_4)_3 \cdot 18H_2O$, 99%), titanium dioxide (TiO_2), alumina (Al_2O_3), ethanol, methanol, ammonia ($NH_3 \cdot H_2O$), concentrated sulfuric acid (98%) and hydrogen peroxide solution (H_2O_2) were analytical grade and purchased from Guangzhou Chemical Reagent Factory, China. 4-Vinylpyridine (96%), gold chloride trihydrate ($HAuCl_4 \cdot 3H_2O$, ≥99.9% trace metals basis), $_D$-xylose (98%), toluene, 3-mercaptopropyltrimethoxysilane, ether, acetone and tetraethoxysilane (TEOS) were also analytical grade and obtained from Aladdin Industrial Corporation. $_D$-Xylonic acid calcium salt hydrate was bought from Sigma-Aldrich. SBA-15 was obtained from Nanjing JCNANO Technology Co., Ltd., China. Except for styrene, all the others chemicals were used without further purification. QCM-D sensors with Al_2O_3, silica and gold surface were supplied by Q-Sense AB (Biolin Scientific Co. Ltd, Sweden).

Synthesis of Au/SBA-15 Catalyst: The Au/SBA-15 catalyst was prepared using the procedure which has been reported previously[1] with slight modification. An aqueous solution of $HAuCl_4 \cdot 3H_2O$ was stirred at room temperature. The required amount of SBA-15 was added into the solution and then the system was stirred for 4 h. After that, a certain amount of 0.1 mol/L freshly prepared $NaBH_4$ aqueous solution was added dropwise to the above solution, and the solution was stirred for another period time. Finally, the solid product was filtered, washed thoroughly with deionized water until the filtrate contained no chloride ions (confirmed with $AgNO_3$ test) and then dried in a vacuum oven at 60 °C. The catalyst was calcined at 400 ^oC for 3 h before use.

Synthesis of Au/Al_2O_3 Catalyst: The Au/Al_2O_3 catalyst was prepared using the procedure which has been reported previously[2] with slight modification. The aqueous solution of $HAuCl_4 \cdot 3H_2O$ was stirred at 500 rpm, and then 0.1 mol/L sodium hydroxide solution was added dropwise until the pH of the solution reached 7. After that, the requisite amount of Al_2O_3 was added to the solution, and the reaction system was carried out at 50 ^oC for 1 h under stirring. Finally, the catalyst was washed with water to remove Cl^-, dried at 60 ^oC overnight and calcined at 400 ^oC for 3 h.

Synthesis of SiO_2-SH-Au Catalyst: In a typical procedure, a mixture of ethanol (100 mL), water (2 mL) and ammonia (5 mL) was stirred at 40 ^oC for 2 h. Thereafter, 8 mL tetraethoxysilane (TEOS) was added dropwise to the solution, and the mixture was then stirred for 24 h. After that, the mixture was cooled to room temperature, centrifuged (6000 rpm, 10 min), and the obtained solid was re-dispersed in ethanol, and then centrifuged (6000 rpm, 10 min). This procedure was repeated for 3 times. Finally, the obtained white solid was dried in a vacuum oven at 90 °C for 24 h. In order to increase the amount of -OH on the surface of SiO_2 and remove the organic component of SiO_2, the dried SiO_2 was soaked in the mixture of hydrogen peroxide and concentrated sulfuric acid for a period of time. Finally, the surface-treated SiO_2 was centrifuged, washed and dried in a vacuum oven at 120 ^oC.

0.5 g surface-treated SiO_2 was added to 50 mL of toluene and the mixture was subjected to sonication for 30 min. Thereafter, 2 mL 3-mercaptopropyltrimethoxysilane was added dropwise to the solution, and the reaction system was carried out at 110 ^oC for 24 h. After that, the mixture was cooled to room temperature, filtered, washed with toluene,

ether, acetone and methanol to remove the free 3-mercaptopropyltrimethoxysilane. The final product of SiO_2-SH was obtained by drying at 60 ^oC in a vacuum oven.

The requisite amount of SiO_2-SH was added to the aqueous solution of $HAuCl_4 \cdot 3H_2O$, and the reaction was carried out at 60 ^oC for a period of time. Thereafter, 25 mL of ethanol was added to the above mixture, followed by stirring for another 18 h at 60 ^oC. After cooling to room temperature, the SiO_2-SH-Au catalyst was filtered, washed with ethanol, and dried in a vacuum oven at 60 ^oC.

Synthesis of C-SH-Au Catalyst: The C microspheres were synthesized by hydrothermal method. In a typical procedure, 1 g of $_D$-xylose was dissolved in 30 mL of water. Then the mixture was transferred into an autoclave and kept still at 220 ^oC for 12 h. After cooling to room temperature, the C microspheres were isolated by centrifugation and washed with water and ethanol, dried in a vacuum oven at 60 ^oC.

0.5 g C microspheres were added to 50 mL of toluene and the mixture was subjected to sonication for 30 min. Thereafter, 2 mL 3-mercaptopropyltrimethoxysilane was added dropwise to the solution, and the reaction system was carried out at 110 ^oC for 24 h. After that, the mixture was cooled to room temperature, filtered, washed with toluene, ether, acetone and methanol to remove the free 3-mercaptopropyltrimethoxysilane. The final product of C-SH was obtained by drying at 60 ^oC in a vacuum oven.

The requisite amount of C-SH was added to the aqueous solution of $HAuCl_4 \cdot 3H_2O$, and the reaction was carried out at 60 ^oC for a period of time. Thereafter, 25 mL of ethanol was added to the above mixture,

followed by stirring for another 18 h at 60 ^{o}C. After cooling to room temperature, the C-SH-Au catalyst was filtered, washed with ethanol, and dried in a vacuum oven at 60 ^{o}C.

Catalysts Characterization: X-ray diffraction (XRD) patterns were obtained using a Bruker D8 Focus Diffractometer equipped with Cu Kα radiation (λ = 0.15418 nm) scanned from 30^{o} to 90^{o}. The voltage and current were 40 kV and 40 mA, respectively. Scanning electron microscope (SEM) images were derived on a Zeiss EVO 18 (Jena, Germany) operated at a 10 kV acceleration voltage. Transmission electron microscopy (TEM) images were derived on a JEM-2100 (HR) operated at a 200 kV acceleration voltage. XPS measurements were conducted on a Kratos Axis Ultra DLD spectrometer employing amonochromated Al Kα X-ray source (hν = 1486.6 eV). Inductively coupled plasma atomic emission spectroscopy (ICP-MS) was performed on Agilent 7700 equipment. Thermogravimetric analysis (TGA) was performed on a TAQ500 thermogravimetric analyzer. N_2 adsorption-desorption isotherms measurements were performed on an ASAP 2460 volumetric adsorption analyzer at 77 K. The Brunauer-Emmett-Teller (BET) method was used to calculate the specific surface area of all samples. The desorption branch of isotherm in line with the Barrett-Joyner-Halenda method was utilized to evaluate the average pore diameter and pore size distributions of each sample.

Adsorption of $_{D}$-xylose on Al_2O_3, silica, and gold surfaces: Quartz crystal microbalance with dissipation monitoring (QCM-D, Biolin Scientific Co. Ltd, Sweden) was employed to assess the affinity of $_{D}$-xylose to various surfaces. All substrates were subjected to UVO radiation (28 mW/cm^2 at 254 nm) for 15 min, immediately prior to use. QCM sensors were

mounted in the chambers and mili-Q water was loaded to remove impurities of the surfaces and stabilized the system at the rate 0.1 mL/min. The temperature in the chambers was kept at 25 °C during the entire measurements. The $_D$-xylose solution with a concentration of 0.1 mg/mL was loaded into three chambers of QCM at a rate 0.1 mL/min after the QCM system was stabilized. Once the adsorption of $_D$-xylose on Al_2O_3, silica, and gold surfaces reached their equilibrium state, mili-Q water was introduced again to remove the loosely bounded $_D$-xylose on the surfaces. The resulting frequency and dissipation changes of QCM crystals at 5 MHz fundamental resonance frequency and their 3rd, 5th, 7th, 9th, and 11th overtone data were recorded. Since the trend of overtones was similar, only the 3rd overtone data was reported in this paper.

Computational Details: The structure of the $_D$-xylose was optimized by DMOL3 module in Materials Studio 2017[3] with GGA/PW91 basis set in fine quality combined DFT semi-core pseudopots and DFT-D counterpoise correction, which has been widely used adopted in other reports.[4-7] Herein, (110) crystal face is chosen to investigate the adsorption energy of $_D$-xylose on Al_2O_3, which was optimized using Forcite Module in Materials Stuido 2017[3] with an ultrafine basis set by means of smart algorithm, with the parameters sets as $1 \cdot 10^{-5}$ kcal/mol (energy), 0.0005 kcal·mol^{-1}Å^{-1} (forces), and $5.0 \cdot 10^{-6}$ Å (displacement) before calculating adsorption energy. The value of adsorption energy (Ea) was obtained by the equation as follows:[8]

$$E_a = E_{(cry\text{-}xyl)} - E_{cry} - E_{xyl}$$

where $E_{cry\text{-}xyl}$, E_{cry} and E_{xyl} refer to the energy of the optimized adsorption system, crystal face and the adsorbed $_D$-xylose, respectively.

In terms of the O_2 dissociation energy on the interface of Au and Al_2O_3, the structure of Al_2O_3 was constructed by inserting an Au atom into the defect of the framework of Al_2O_3. The structure was preoptimizing by the same method as that for Al_2O_3 and then O_2 molecule was placed near the Au atom. The value of O_2 dissociation energy (Ed) on the interface of Au and Al_2O_3. was generated using the equation as follows:[9]

$$E_d = E_{(cry\text{-}O2)} - E_{cry} - E_{(O2)}$$

where $E_{(cry\text{-}O2)}$, E_{cry} and E_{O2} represent the energy of the optimized crystal with dissociated O_2 molecule, crystal structure and O_2 molecule, respectively.

Catalytic Activity Test: The catalytic synthesis of $_D$-xylonic acid were carried out in a 60 mL Teflon-lined stainless-steel autoclave. In a typical procedure, 0.25 g $_D$-xylose was dissolved in 25 mL water, and then a certain amount of Au@*h*-Al_2O_3 was added into the solution and dispersed by ultrasound for 10 min. Then oxygen was purged into the reactor for three times before the reactor being sealed and pressurized with oxygen. The reaction was then heated to a required temperature for different times under constant stirring (1000 rpm). After the completion of the reaction, the autoclave was immersed in a water bath to cool down, and the oxygen was expelled from the stainless-steel autoclave at the same time. Finally, the sample was immediately syringed out, filtered and analyzed by high-performance liquid chromatography (HPLC, Agilent 1260 series) with a UV detector.

Similar methods were used for the catalyst studies. In all cases, the catalysts were recovered after reaction by centrifuging for 5 min (8000

rpm). The solid was washed with distilled water for several times until the supernatant became neutral. The washed catalysts were dried at 80 °C for at least 10 h prior to reuse. Furthermore, other catalysts for the synthesis of D-xylonic acid were similar to the procedure catalyzed by Au@*h*-Al_2O_3.

Product detection: All the samples were immediately syringed out, filtered and analyzed by high-performance liquid chromatography (HPLC, Agilent 1260 series) with a UV detector at 210 nm and a Bio-Rad Aminex HPX-87H column (300 mm × 7.8 mm × 9 μm). A 5 mM H_2SO_4 mobile phase was employed as the mobile phase at 55 °C with a flow rate of 0.6 mL min^{-1}. D-Xylose was quantitated using a High Performance Ion Chromatography (HPIC, Dionex ICS-3000) system with an integrated amperometric detector and a CarboPac PA1 column at 30 °C using pure water as an eluent. The concentrations of the products were determined by comparing the calibration curve established with the external standard. The conversion of D-xylose and the yields of the products were calculated by the following equations:[10]

$$Conversion\ (\%) = \frac{Moles\ of\ carbon\ in\ feedstock\ consumed}{Moles\ of\ carbon\ in\ feedstock\ input} \times 100\%$$

$$Product\ yield\ (\%) = \frac{Moles\ of\ carbon\ in\ organic\ acid}{Moles\ of\ carbon\ in\ feedstock\ input} \times 100\%$$

The possible reaction pathway for the base-free oxidation of D-xylose catalyzed by Au/Al_2O_3 and Au@PS-co-P4VP@Al_2O_3: In this work, the

other products of formic acid, acetic acid and lactic acid were given in Table S7 during the catalysis processes of Au/Al_2O_3 and Au@PS-co-P4VP@Al_2O_3. We then proposed possible mechanisms through these results and related literature.[10-13] The possible reaction pathway for the base-free oxidation of D-xylose catalyzed by Au/Al_2O_3 was shown in Fig. S16. First, the ring opening reaction of D-xylose molecules generates the intermediate 1. The aldehyde group on the intermediate Ⅰ was oxidized to carboxyl group, producing D-xylonic acid. Meanwhile, the isomerization reaction of the intermediate 1 generates the intermediate Ⅱ. Similar "retro-aldol" reaction of intermediate 2 was carried out to give dihydroxyacetone and intermediate Ⅲ. The lactic acid could be produced by isomerization and dehydration of dihydroxyacetone, respectively. Furthermore, the oxidative α-dicarbonyl cleavage of intermediate Ⅴ could be giving acetic acid. In addition, the α-oxidation and β-oxidation of intermediate Ⅰ and D-xylonic acid were performed to give the final product of formic acid, respectively. As we known, the content of formic acid in the byproduct is higher than others, therefore, the α-oxidation and β-oxidation of intermediate Ⅰ and D-xylonic acid take precedence over other steps during the side reaction. As shown in the Table S7 and Fig. S17, the content of lactic acid in the byproduct is higher than others. Thus, the process of lactic acid production is priority during the side reaction. Similarly, the ring opening of D-xylose was first performed to give intermediate Ⅰ. Then the isomerization of intermediate Ⅰ generates intermediate Ⅱ. Similar "retro-aldol" reaction intermediate 2 was carried out to give dihydroxyacetone and intermediate Ⅲ. the isomerization and dehydration of dihydroxyacetone were performed to give the final

product of lactic acid, respectively. Meanwhile, the intermediate Ⅲ can be further reacted to form formic acid.

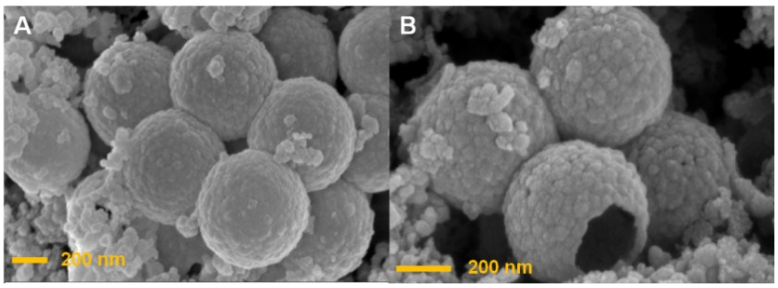

Fig. S1 SEM of Au@*h*-Al_2O_3 (A, B).

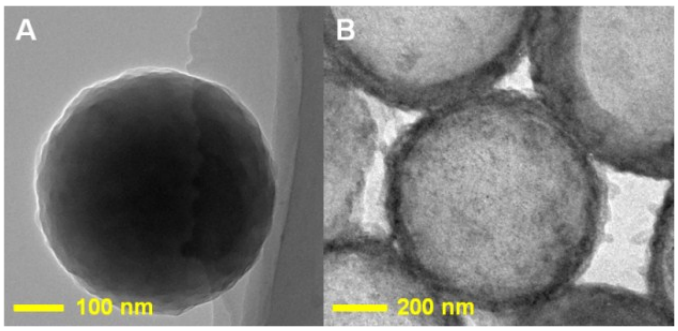

Fig. S2 TEM of PS-*co*-P4VP (A) and Au@PS-*co*-P4VP@Al_2O_3 (B).

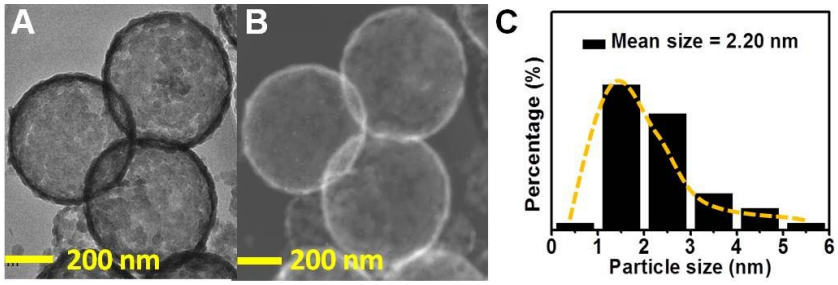

Fig. S3 TEM (A) and STEM (B) of 10th reused of Au@*h*-Al_2O_3 for 10th reuse. (C) The size distribution of 10th reused Au NPs from 300 particles.

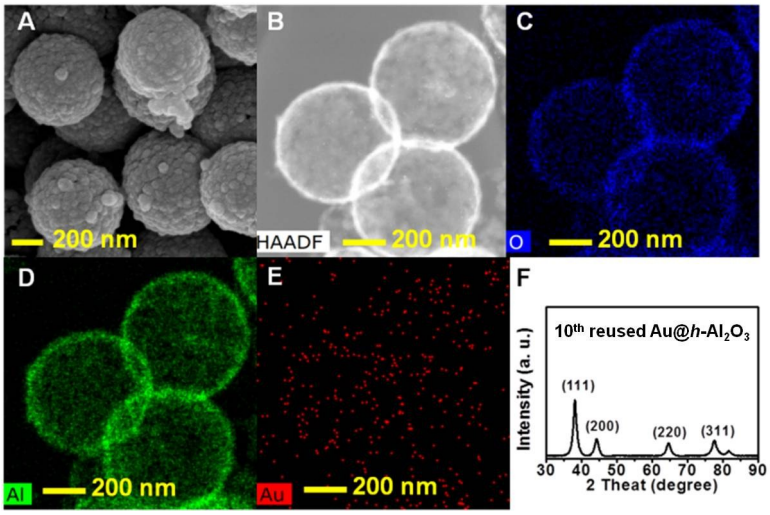

Fig. S4 SEM of 10th reused of Au@*h*-Al_2O_3. (B) HAADF-STEM of Au@*h*-Al_2O_3 for 10th reuse and element mapping images: (C) O element, (D) Al element, and (E) Au element. (F) The XRD patterns of 10th reused of Au@*h*-Al_2O_3.

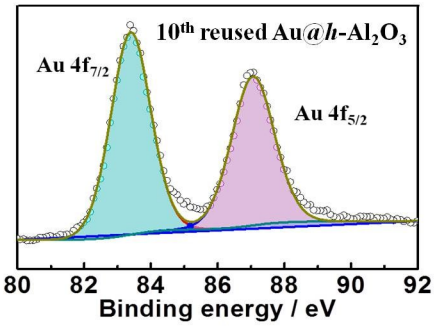

Fig. S5 Au 4f spectrum for 10th-reused Au@*h*-Al_2O_3.

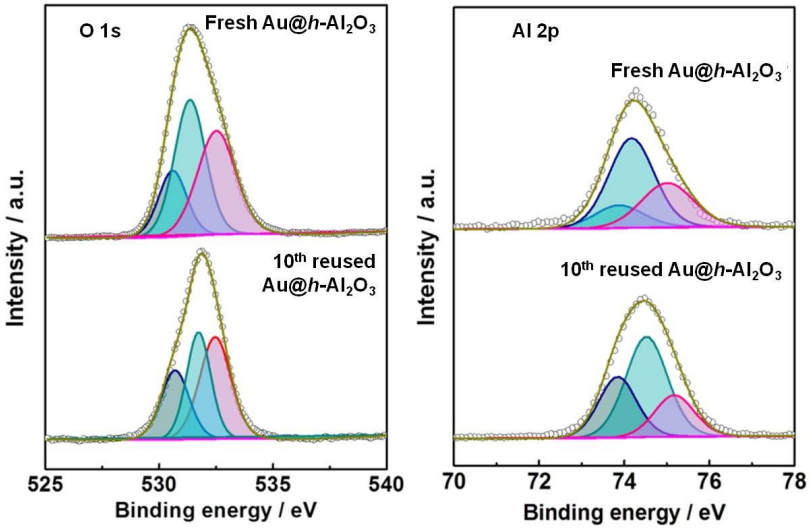

Fig. S6 O (1s) and Al (2p) spectra for fresh Au@*h*-Al_2O_3 and 10^{th} reused Au@*h*-Al_2O_3.

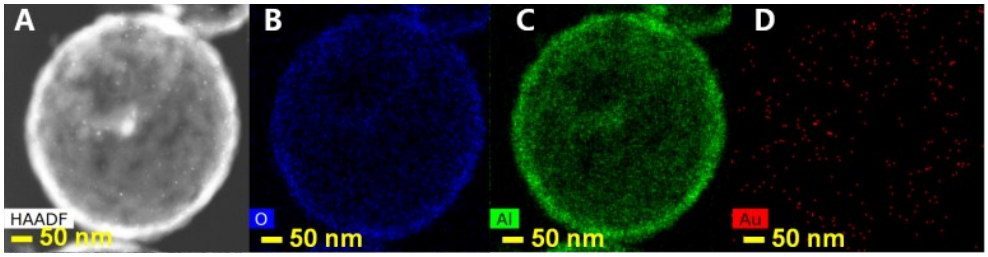

Fig. S7 HAADF-STEM of Au@*h*-Al_2O_3 (A). Element mapping images of Au@*h*-Al_2O_3: (B) O element, (C) Al element, and (D) Au element.

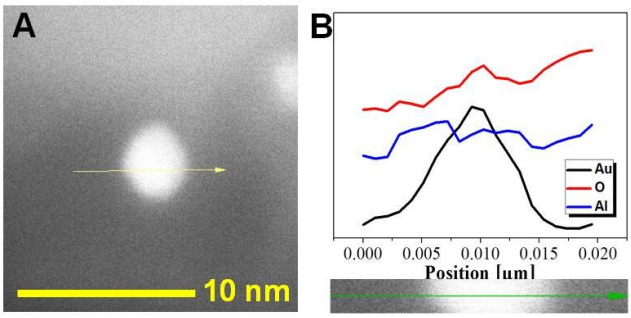

Fig. S8 STEM of Au NP (A) and the line scan of Au@*h*-Al_2O_3 (B).

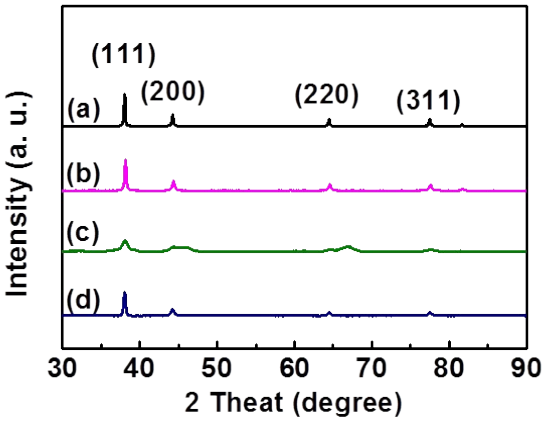

Fig. S9 XRD patten of Au/SBA-15 (a), Au-SH-SiO_2 (b), Au/Al_2O_3 (c), Au-SH-C (d).

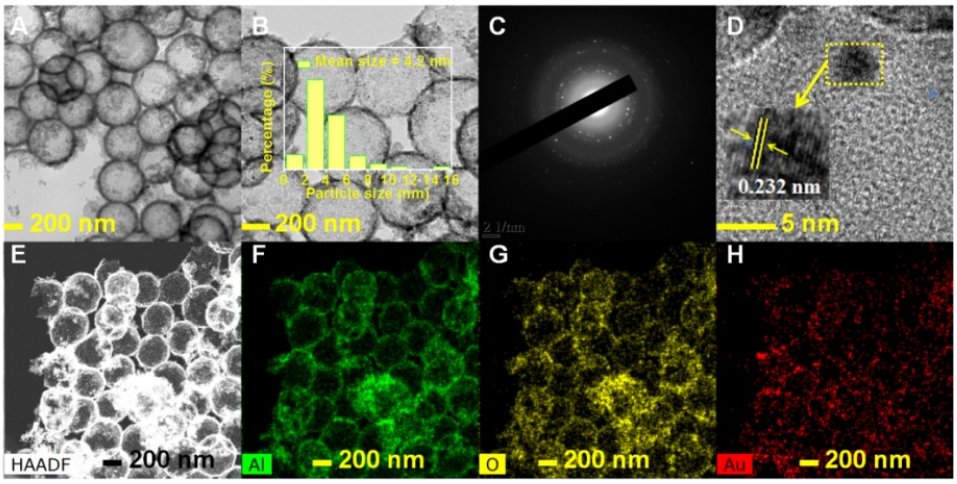

Fig. S10 TEM of Au@*h*-Al_2O_3-10 (A, B, the inset is Au nanoparticle size distributions based on 300 particles)). (C) Diffraction patterns of Au nanoparticles. (D) High-resolution TEM image of Au@*h*-Al_2O_3-10. (E) STEM-HAADF image of Au@*h*-Al_2O_3-10 and element mapping images of Au@*h*-Al_2O_3-10: (F) Au element, (G) O element, and (H) Al element.

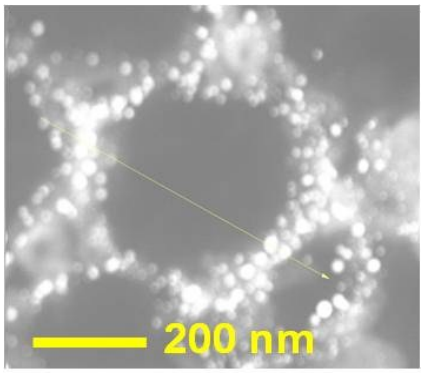

Fig. S11 The STEM of cross section diagram of Au@*h*-Al_2O_3-10.

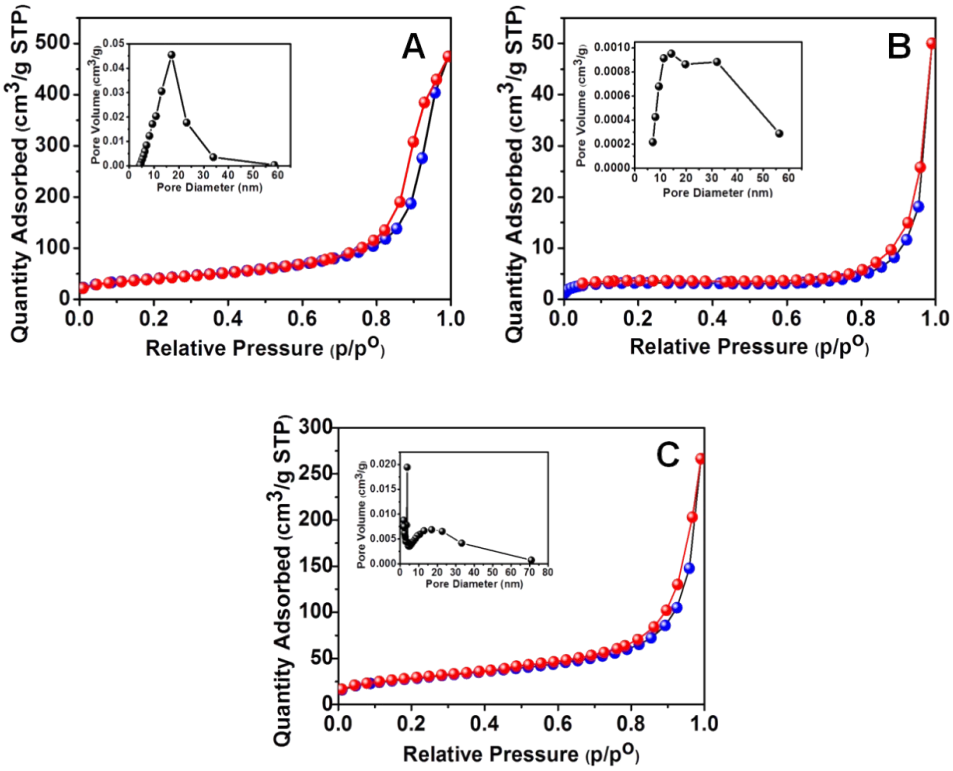

Fig. S12 Nitrogen adsorption isotherm of the Au/Al_2O_3 (A), Au@PS-*co*-P4VP@Al_2O_3 (B) and Au@*h*-Al_2O_3 (C). The insert image represents the BJH pore size distribution of Au/Al_2O_3, Au@PS-*co*-P4VP@Al_2O_3 and Au@*h*-Al_2O_3.

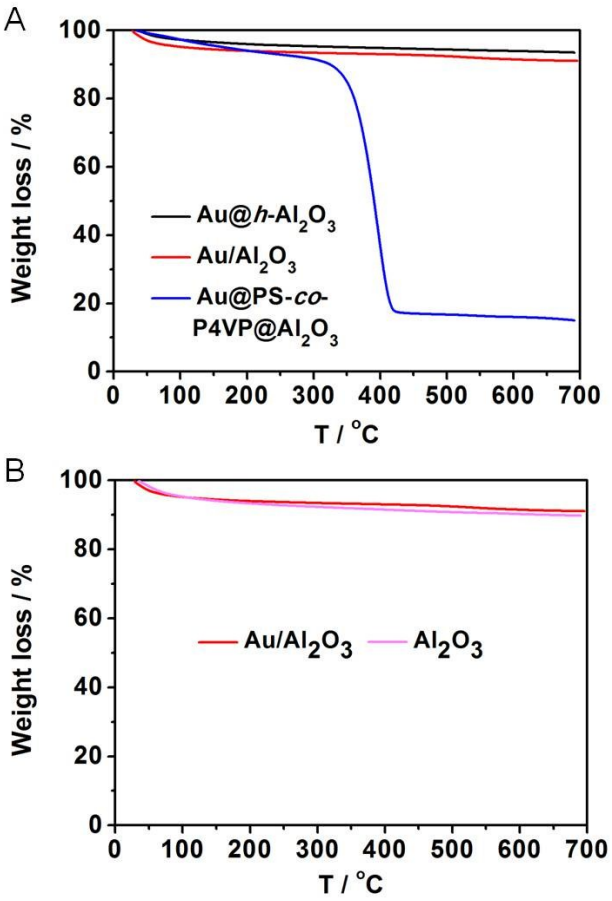

Fig. S13 (A) TGA curves of Au/Al_2O_3, $Au@h\text{-}Al_2O_3$ and $Au@PS\text{-}co\text{-}P4VP@Al_2O_3$; (B) TGA curves of Au/Al_2O_3 and Al_2O_3.

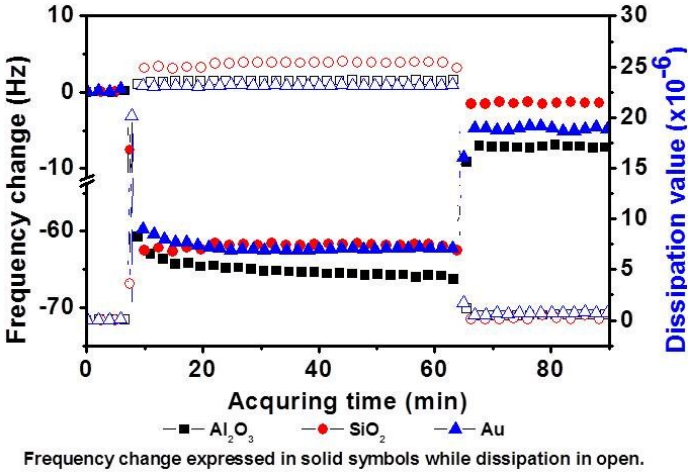

Fig. S14 The affinities of $_D$-xylose to various surfaces (Al_2O_3, silica, and gold) by a technique of quartz crystal microbalance with dissipation monitoring (QCM-D).

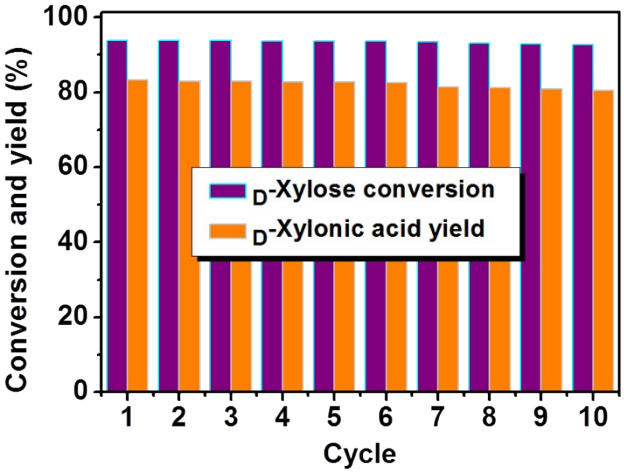

Fig. S15 Recycle of Au@*h*-Al_2O_3.

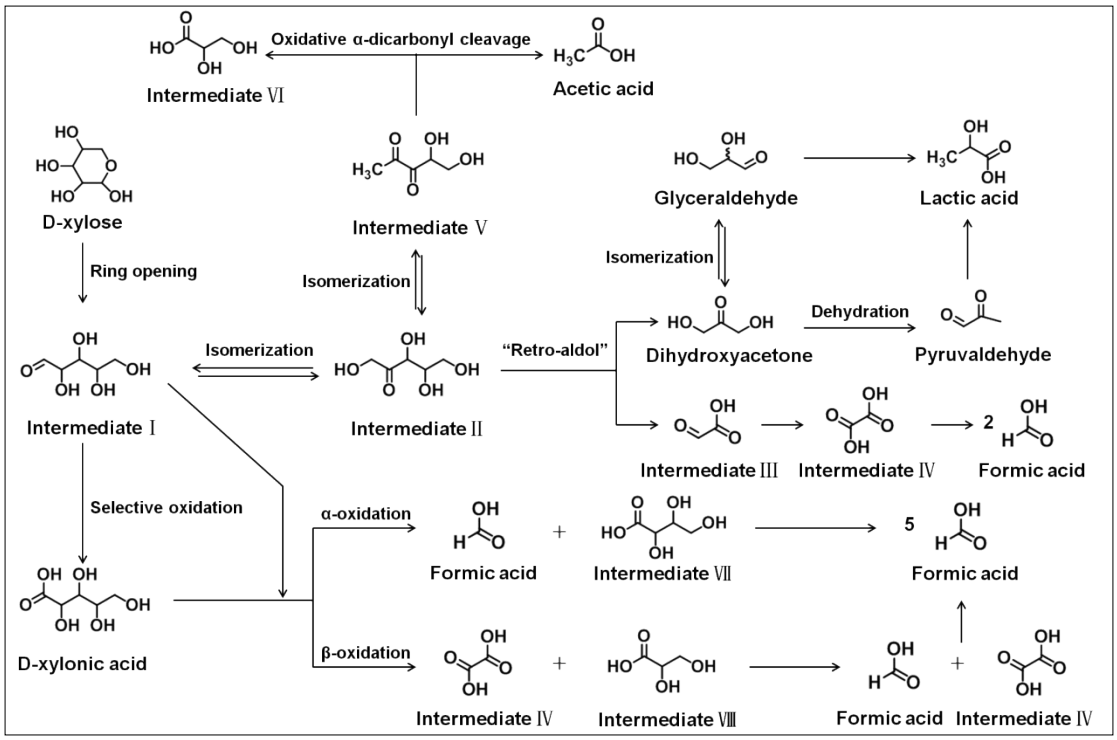

Fig. S16 The possible reaction pathway for the base-free oxidation of D-xylose catalyzed by Au/Al_2O_3.

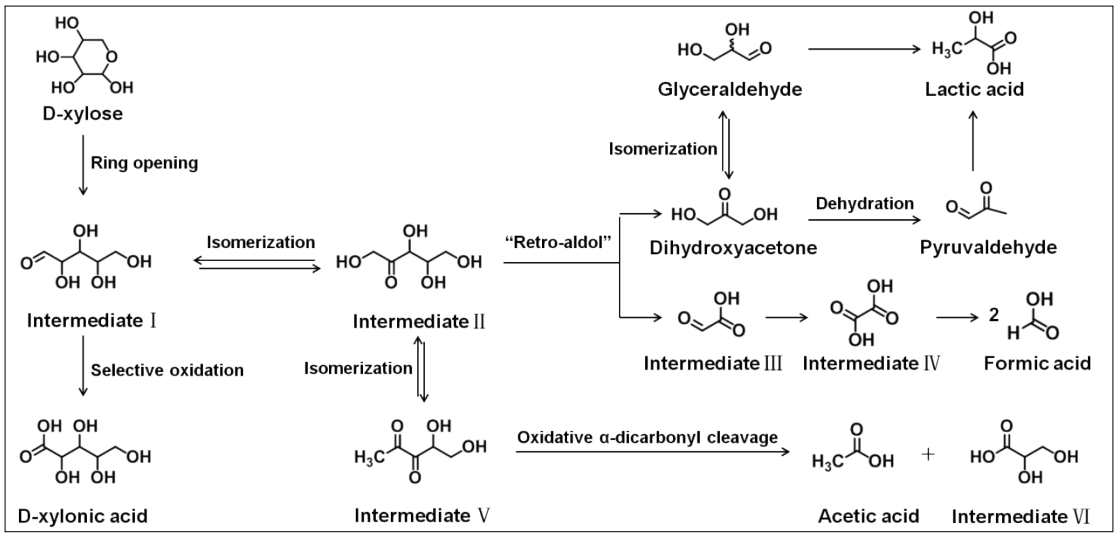

Fig. S17 The possible reaction pathway for the base-free oxidation of D-xylose catalyzed by Au@PS-*co*-P4VP@Al_2O_3.

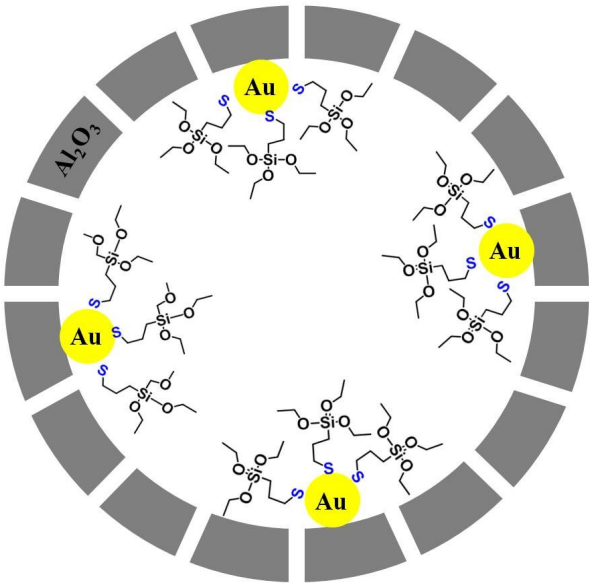

Fig. S18 The model of Au-SH-$(CH_2)_3$-Si$(OCH_3)_3$@*h*-Al_2O_3.

Table S1. The Au content was measured by ICP-MS.[a]

Entry	Sample	Au content (wt%)
1	Au@*h*-Al_2O_3	2.80
2	10^{th}-reused Au@*h*-Al_2O_3	2.49
3	Au/Al_2O_3	2.81
4	Au/SBA-15	2.77
5	Au@PS-*co*-P4VP	2.80
6	SiO_2-SH-Au	2.79
7	C-SH-Au	2.75

[a] Inductively Coupled Plasma Mass Spectrometer.

Table S2. Catalytic behaviours of Au@*h*-Al_2O_3 for base-free oxidation of $_D$-xylose under different temperatures.[a]

Entry	Temperature (^oC)	Conversion (%)	Yield (%)				
			$_D$-Xyloni c acid	Formi c acid	Aceti c acid	Lacti c acid	Others [b]
1	100	85.9	38.6	Trace	13.9	20.3	13.1
2	110	86.5	49.8	Trace	10.5	19.0	7.2
3	120	87.0	64.0	1.4	9.6	11.2	0.8
4	130	93.8	83.3	6.3	3.8	Trace	0.4
5	140	99.0	70.2	11.9	3.1	1.7	12.1
6	150	100	63.2	10.3	7.5	4.3	14.7
7	160	100	39.5	12.3	10.5	8.0	29.7

[a] Typical reaction conditions: $_D$-xylose (0.25 g), O_2 (3.0 MPa), Au@*h*-Al_2O_3 (20 mg), water (25 mL), and 60 min, [b] uncertain byproducts and losses in these processes.

Table S3. Catalytic behaviours of Au@*h*-Al_2O_3 for base-free oxidation of D-xylose under different oxygen pressures.[a]

Entry	O_2 (MPa)	Conversion (%)	Yield (%)				
			D-Xylonic acid	Formic acid	Acetic acid	Lactic acid	Others[b]
1	0	85.3	14.7	Trace	16.0	8.7	45.9
2	1.0	87.9	49.7	Trace	6.9	12.9	18.4
3	1.5	88.6	60.9	1.1	5.4	10.2	11
4	2.0	89.1	70.2	1.2	6.0	10.9	0.8
5	2.5	89.9	75.6	2.9	6.7	4.3	0.4
6	3.0	93.8	83.3	6.3	3.8	Trace	0.4
7	4.0	95.3	79.6	11.8	2.2	Trace	1.7

[a] Typical reaction conditions: D-xylose (0.25 g), Au@*h*-Al_2O_3 (20 mg), water (25 mL), 60 min, and 130 °C, [b] uncertain byproducts and losses in these processes.

Table S4. Catalytic behaviours of Au@*h*-Al_2O_3 for base-free oxidation of D-xylose under different catalyst dosages.[a]

Entry	Cat. Dosage (mg)	Conversion (%)	Yield (%)				
			D-Xylonic acid	Formic acid	Acetic acid	Lactic acid	Others[b]
1	2.5	86.8	31.1	Trace	16.7	6.4	32.6
2	5.0	87.4	48.1	3.0	13.2	6.0	17.1
3	10.0	91.5	62.2	3.4	11.9	5.3	8.7
4	20.0	93.8	83.3	6.3	3.8	Trace	0.4
5	30.0	100	78.2	7.1	7.5	5.4	1.8

[a] Typical reaction conditions: D-xylose (0.25 g), O_2 (3.0 MPa), water (25 mL), 60 min, and 130 °C, [b] uncertain byproducts and losses in these processes.

Table S5. Catalytic behaviours of Au@*h*-Al_2O_3 for base-free oxidation of $_D$-xylose under different reaction times.[a]

Entry	Time (min)	Conversion (%)	Yield (%)				
			$_D$-Xylonic acid	Formic acid	Acetic acid	Lactic acid	Others[b]
1	10	88.6	58.0	Trace	5.2	5.8	19.6
2	30	90.2	66.5	2.2	8.8	3.7	9.0
3	45	91.4	73.4	2.9	11.4	3.1	0.6
4	60	93.8	83.3	6.3	3.8	Trace	0.4
5	90	95.3	76.4	6.5	9.5	Trace	2.9
6	120	95.5	66.1	8.4	15.1	Trace	5.9

[a] Typical reaction conditions: $_D$-xylose (0.25 g), O_2 (3.0 MPa), water (25 mL), Au@*h*-Al_2O_3 (20 mg), and 130 ^oC, [b] uncertain byproducts and losses in these processes.

Table S6. Base-free oxidation of $_D$-xylose catalyzed by different Au catalysts.[a]

Entry	Catalyst	$_D$-Xylose conversion (%)	$_D$-Xylonic acid (%)
1	Au/SBA-15	85.7	16.8
2	Au@PS-*co*-P4VP	84.7	11.4
3	SiO_2-SH-Au	85.1	11.6
4	C-SH-Au	82.3	10.8

[a] Typical reaction conditions: $_D$-xylose (0.25 g), O_2 (3.0 MPa), water (25 mL), Au based catalyst (20 mg), 130 ^oC, and 60 min.

Table S7. The yields of byproducts catalyzed with different Al_2O_3-based Au catalyst for the base-free oxidation of $_D$-xylose.[a]

Entry	Al_2O_3-based Au catalyst	Dihydroxy acetone	Formic acid	Acetic acid	Lactic acid	Others[b]
1	Au/Al_2O_3	7.8%	26.7%	14.0%	9.2%	10.7%
2	Au@PS-*co*-P4VP@Al_2O_3	7.2%	6.6%	13.5%	23.4%	14.2%
3	Au@*h*-Al_2O_3	Trace	6.3%	3.8%	Trace	0.4%

[a] Typical reaction conditions: $_D$-xylose (0.25 g), O_2 (3.0 MPa), water (25 mL), Al_2O_3-based Au catalyst (20 mg), 130 ^oC, 60 min, [b] uncertain byproducts and losses in these processes.

Supplementary Information References:

1 A. Kumar, V. P. Kumar, A. Srikanth, V. Vishwanathan and K. V. R. Chary, *Catal. Lett*., 2016, **146**, 35.

2 A. V. Chistyakov, P. A. Zharova, S. A. Nikolaev and M. V. Tsodikov, *Catal. Today*, 2017, **279**, 124.

3 Dassault Systèmes BIOVIA, Materials Studio 2017, San Diego: Dassault Systèmes, 2017.

4 Z. F. Yan, J. Y. Fan, Z. J. Zuo, Z. Li and J. S. Zhang, *Appl. Surf. Sci*., 2014, **288**, 690.

5 L. X. Ling, M. H. Fan, B. J. Wang and R. G. Zhang, *Energy. Environ. Sci*., 2015, **8**, 3109.

6 F. Z. Liu, C. Wu, G. Yang and S. C. Yang, *J. Phys. Chem. C*., 2015, **119**, 15500.

7 L. L. Gong, X. F. Feng, F. Luo, X. F. Yi and A. M. Zheng, *Green Chem*., 2016, **18**, 2047.

8 S. S. Laletina, M. Mamatkulov, E. A. Shor, V. V. Kaichev, A. Genest, I. V. Yudanov and N. Rosch, *J. Phys. Chem. C*, 2017, **121**, 17371.

9 S. Roy, V. Mujica and M. A. Ratner, *J. Chem. Phys*., 2013, **139,** 1.

10 H. D. Zhang, N. Li, X. J. Pan, S. B. Wu and J. Xie, *Green Chem*., 2016, **18**, 2308.

11 W. J. Dong, Z. Shen, B. Y. Peng, M. Y. Gu, X. F. Zhou, B. Xiang, Y. L. Zhang, *Sci. Rep.*, 2016, **6**, 1-8.

12 X. Lei, F. F. Wang, C. L. Liu, R. Z. Yang, W. S. Dong, *Appl. Catal. A-Gen*., 2014, **482**, 78-83.

13 P. Wattanapaphawong, O. Sato, K. Sato, N. Mimura, P. Reubroycharoen, A. Yamaguchi, *Catalysts*, 2017, **7**, 1-10.